

Ice thickness over the southern limit of the Amery Ice Shelf, East Antarctica, and reassessment of the mass balance of the central portion of the Lambert Glacier–Amery Ice Shelf system

Jiahong WEN,¹ Long HUANG,¹ Weili WANG,² T.H. JACKA,³ V. DAMM,⁴ Yan LIU⁵

¹*Department of Geography, Shanghai Normal University, Shanghai, China*
E-mail: jhwen@shnu.edu.cn

²*SGT Inc., NASA Goddard Space Flight Center, Greenbelt, MD, USA*

³*Antarctic Climate and Ecosystems Cooperative Research Centre, Hobart, Tasmania, Australia*

⁴*Federal Institute for Geosciences and Natural Resources, Hannover, Germany*

⁵*College of Global Change and Earth System Science & State Key Laboratory of Remote Sensing Science, Beijing Normal University, Beijing, China*

ABSTRACT. We combine radio-echo sounding ice thickness data from the BEDMAP Project database and the PCMEGA (Prince Charles Mountains Expedition of Germany and Australia) dataset to generate a new ice thickness grid for the southern limit region of the Amery Ice Shelf, East Antarctica. We then reassess the mass balance of the central portion of the Lambert–Amery system, incorporating flow information derived from synthetic aperture radar interferometry (InSAR) and a modeled surface mass-balance dataset based on regional atmospheric modeling. Our analysis reveals that Mellor and Fisher Glaciers are approximately in balance to the level of our measurement uncertainty, while Lambert Glacier has a positive imbalance of $4.2 \pm 2.3 \text{ Gt a}^{-1}$. The mass budget for the whole Lambert Glacier basin is approximately in balance, and the average basal melt rate in the downstream section of the ice shelf is $5.1 \pm 3.0 \text{ m a}^{-1}$. Our results differ substantially from other recent estimates using hydrostatically derived ice thickness data.

KEYWORDS: Antarctic glaciology, ice-sheet mass balance

INTRODUCTION

The Lambert Glacier–Amery Ice Shelf system, ~10% of the entire Antarctic ice sheet, is one of the largest glacier/ice-shelf systems in Antarctica. It is an important drainage basin in terms of the overall mass balance of the ice sheet and has been the focus of attention for understanding the response of the ice sheet to present and future climate change. The central portion of the system consists of Lambert, Mellor and Fisher glaciers, which drain into the Amery Ice Shelf at its southern limit and then become the central flowbands within the ice shelf (Budd and others, 1982; Wen and others, 2007; Fig. 1a). Amery Ice Shelf, with a length of ~560 km, has an area of ~60 820 km² (Yu and others, 2010). The basin of the three glaciers, i.e. the grounded area of the central portion of the system, which corresponds to the Lambert Glacier basin as defined by Rignot (2002), has an area of $\sim 0.97 \times 10^6 \text{ km}^2$ (Wen and others, 2007) and covers ~70% of the entire Amery drainage basin. The three glaciers contribute significantly to the mass budget of the Lambert–Amery system (Allison, 1979; Yu and others, 2010).

Several previous studies have focused on the mass budget of the Lambert Glacier basin (e.g. Allison, 1979; McIntyre, 1985; Bentley and Giovinetto, 1991; Fricker and others, 2000; Rignot, 2002; Wen and others, 2007; Yu and others, 2010). The most recent three studies (Rignot, 2002; Wen and others, 2007; Yu and others, 2010) use similar horizontal ice velocity measurements and the location of the southern grounding line derived by interferometric synthetic aperture radar (InSAR) (Rignot, 2002; Jezek, 2003, 2008; Fricker and others, 2009; Rignot and others, 2011). However, the ice thickness data used to estimate ice fluxes through the southern grounding line are from different sources. The ice

thickness data used by Rignot (2002) and Wen and others (2007) are estimated from surface elevation data using hydrostatic equilibrium calculations. Those used by Yu and others (2010) are based on a 400 m ice thickness grid interpolated from measurements collected by Australian and Russian aerial radio-echo sounding (RES) surveys during 1968–96, and compiled by the British Antarctic Survey BEDMAP Project (Lythe and others, 2001). The total ice fluxes reported for the three glaciers through the southern grounding line of the Amery Ice Shelf are $54.0 \pm 5.4 \text{ Gt a}^{-1}$ (Wen and others, 2007) and $38.9 \pm 3.3 \text{ Gt a}^{-1}$ (Yu and others, 2010) and the reported mass budgets are $-2.6 \pm 6.5 \text{ Gt a}^{-1}$ (Wen and others, 2007) and $12.6 \pm 4.7 \text{ Gt a}^{-1}$ (Yu and others, 2010). The reported basal melt rates near the southern grounding line are $32 \pm 5 \text{ m ice a}^{-1}$ (Rignot, 2002), $31 \pm 5 \text{ m ice a}^{-1}$ (Rignot and Jacobs, 2002), $23.0 \pm 3.5 \text{ m ice a}^{-1}$ (Wen and others, 2007) and $11.4 \pm 2.8 \text{ m ice a}^{-1}$ (Yu and others, 2010). The above mass-balance estimates are based on similar ice velocity and accumulation data. The substantial discrepancies evident in the estimates are thus due primarily to discrepancies within the ice thickness data and therefore require further examination to reduce the mass-balance uncertainties (Yu and others, 2010; Galton-Fenzi and others, 2012). The average ice thickness along the southern grounding line was estimated from hydrostatic considerations to be 2550 m (Wen and others, 2007). The RES average ice thickness, however, is 1291 m (Yu and others, 2010). Yu and others suggest that the uncertainty associated with the sparseness of RES ice thickness data is expected to be reduced by employing the data from the Prince Charles Mountains Expedition of Germany and Australia (PCMEGA) during the 2002/03 austral summer (Damm, 2007).

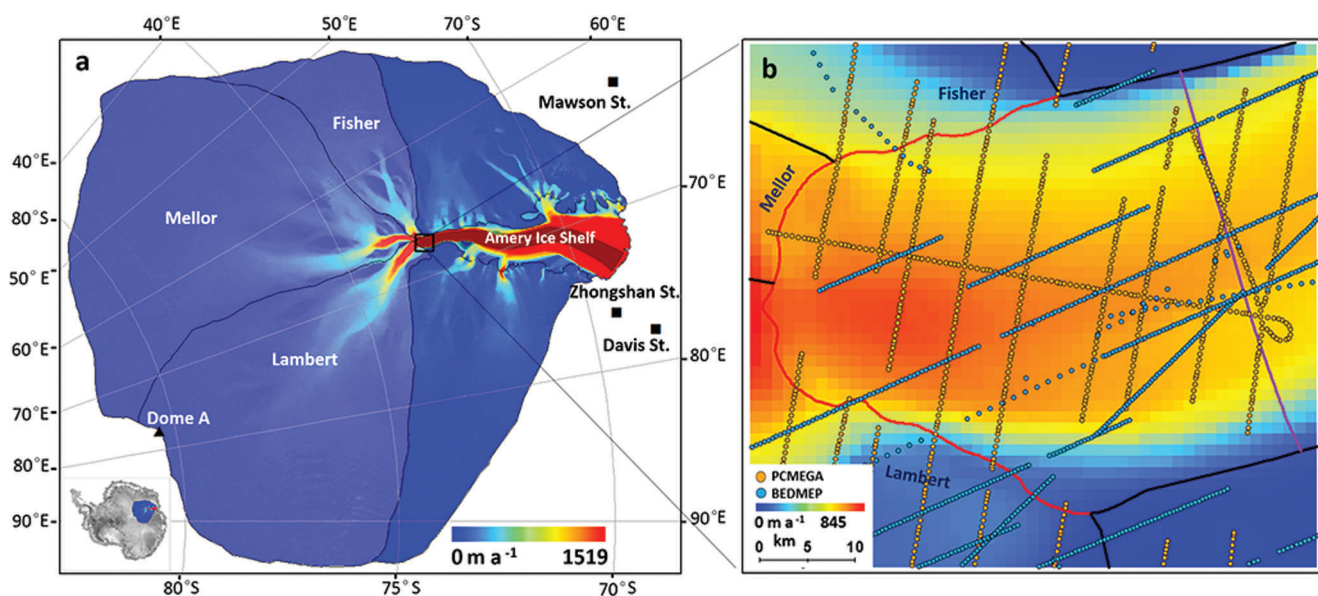


Fig. 1. Maps showing study areas, overlaying a color map showing InSAR surface velocity. (a) The central portion of the Lambert–Amery system, consisting of Lambert, Mellor and Fisher glaciers (in light blue) and their flowbands (in dark red). (b) Ice thickness data from BEDMAP (blue) and PCMEGA (orange) projects in the southern grounding line region of the Amery Ice Shelf. The southern grounding line is shown in red. The G1 flux gate is the pink line.

In this paper, we use ArcGIS to generate a new ice thickness grid over the southern extremity of the Amery Ice Shelf, using the ice thickness data from PCMEGA and BEDMAP, and then combine this gridded ice thickness with a new, high-resolution surface mass-balance (SMB) dataset based on regional atmospheric climate modeling (Lenaerts and others, 2012) to reassess the mass budgets of Lambert, Mellor and Fisher glaciers, and the basal melting beneath the Amery ice Shelf. Our final objective is to provide a more precise assessment of the mass balance for the central portion of the Lambert–Amery system.

DATA

Our datasets include (1) RES ice thickness data, (2) SMB data, (3) InSAR velocities and (4) grounding line data.

Ice thickness data

The ice thickness data from the PCMEGA aerogeophysical campaign and BEDMAP are used to generate a gridded ice thickness over the southern limit region of the Amery Ice Shelf. The region, 1965.7 km² in area, covers the confluence of Lambert, Mellor and Fisher glaciers, which drain across the southern grounding line, into the ice shelf (Fig. 1b).

A grid of flight paths spaced 5 km apart, over a total length of 30 000 km and covering an area of ~100 000 km² ranging from 73° S to 77.5° S and 60° E to 70° E was flown during PCMEGA (Damm, 2007). A 150 MHz pulse radar was used to measure the ice thickness along the flight paths, with a spacing of 10–15 m between signal reflection points. Vertical resolution in ice is 1, 5 or 50 m, depending on selected pulse length.

A total of 745 original survey measurements of ice thickness for the southern extremity of the Amery Ice Shelf were extracted from the BEDMAP dataset (http://www.antarctica.ac.uk/bas_research/data/access/bedmap/) (Fig. 1b). These airborne RES ice thickness data were acquired by the Australian National Antarctic Research

Expeditions (ANARE) during 1972/73, 1973/74 (Mission 5) and 1989 (Mission 7) and by the Soviet Antarctic Expeditions (SAE) during 1987/88 (Mission 70), with measurement errors between 30 and 100 m (Lythe and others, 2001).

In addition, we use ice thickness grids from BEDMAP and BEDMAP2 to compare with our ice thickness results over the southern limit of the Amery Ice Shelf. In 2001, BEDMAP compiled ice thickness measurements from the Antarctic ice sheet collected prior to the 1990s to generate an ice thickness grid, with a spatial resolution of 5 km (Lythe and others, 2001). BEDMAP2 recently presented a new gridded ice-thickness dataset for the Antarctic south of 60° S, using 25 × 10⁶ measurements, over two orders of magnitude more than were used in BEDMAP (Fretwell and others, 2013). BEDMAP2 initially gridded the in situ measurements of ice thickness at 5 km, then the final 1 km ice thickness grid was resampled from the 5 km grid (Fretwell and others, 2013).

Surface mass balance

A new, high-resolution (27 km) SMB dataset for the Antarctic ice sheet is generated, based on output of a regional atmospheric climate model RACMO2.1/ANT, which includes snowdrift physics and is forced by the most recent reanalysis data from the European Centre for Medium-Range Weather Forecasts (ECMWF), ERA-Interim (1979–2010) (Lenaerts and others, 2012). The modeled SMB agrees very well with 750 in situ SMB observations ($R=0.88$; Lenaerts and others, 2012). The SMB dataset shows low SMB values in large parts of the interior ice sheet (<25 mm a⁻¹).

InSAR velocity

The velocity (Fig. 1) and velocity azimuth measurements used in this study are taken from the processed InSAR velocity database (Jezek, 2008; <http://bprc.osu.edu/rsl/radarsat/data/>) with a gridcell size of 400 m. In 2000, three repeat-cycle InSAR data were acquired by a C-band synthetic aperture radar (SAR) sensor on board the RADARSAT-1 satellite during the second Antarctic Mapping Mission (Jezek, 2002, 2003),

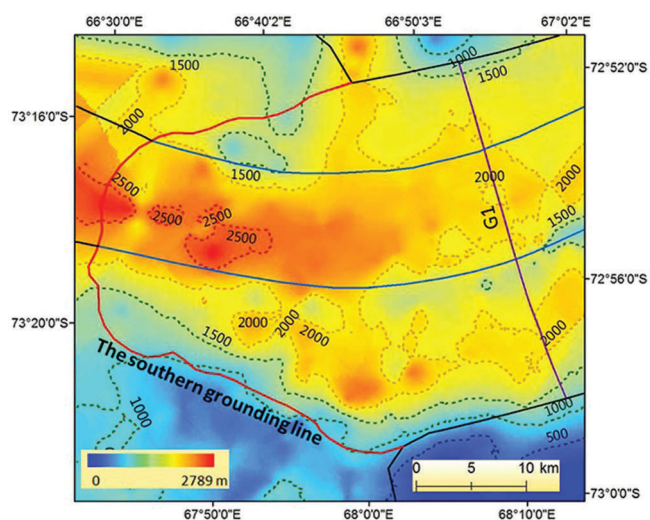


Fig. 2. The ice thickness grid from airborne RES measurements of BEDMAP and PCMEGA, showing the spatial pattern of ice thickness.

also known as the Modified Antarctic Mapping Mission (MAMM). The RADARSAT InSAR data, covering the area from the Antarctic coast to 82° S (Jezek, 2003, 2008), were acquired by a C-band SAR sensor on board the RADARSAT-1 satellite in 2000 (Jezek, 2002, 2003). The GPS velocity measurements over the Amery Ice Shelf over the period 1988–99 (King, 2002; King and others, 2007) were used to compare with the InSAR velocities. The statistics show that the maximum difference between the InSAR velocities and GPS velocity measurements is up to 30 m a⁻¹, and the mean difference is 4.41 ± 9.7 m a⁻¹ (Wen and others, 2010).

Grounding line

The grounding lines of the Antarctic ice sheet have been mapped using satellite visible imagery, altimetry data (e.g. Bindschadler and others, 2011) and differential satellite SAR interferometry (DInSAR) data (Rignot and others, 2011). Here we use the southern grounding line mapping of the Amery Ice Shelf provided by Rignot and others (2011) using DInSAR data from European Remote-sensing Satellites 1 and 2 (ERS-1/2). DInSAR directly measures the vertical motion of floating ice shelves in response to tidal oceanic forcing with millimeter precision at sample spacing <50 m, simultaneously over areas several hundred km wide. This is in contrast to methods that detect abrupt changes in surface slope in satellite visible imagery or altimetry data. The resulting precision of grounding line mapping is 100 m for Lambert Glacier and 300 m for Mellor and Fisher Glaciers (Rignot, 2002).

RESULTS

Ice thickness interpolation

Ninety-four ice thickness outliers from Mission 7 and Mission 70 were removed manually after cross-validation; the standard deviation (1σ) of these ice thickness data is larger than twice the average standard deviation (196 m) of the total samples. The spatial distribution of the ice thickness measurements is characterized by dense sampling along-track while the flight tracks themselves are widely spaced. Such a distribution poses difficulties for most interpolation

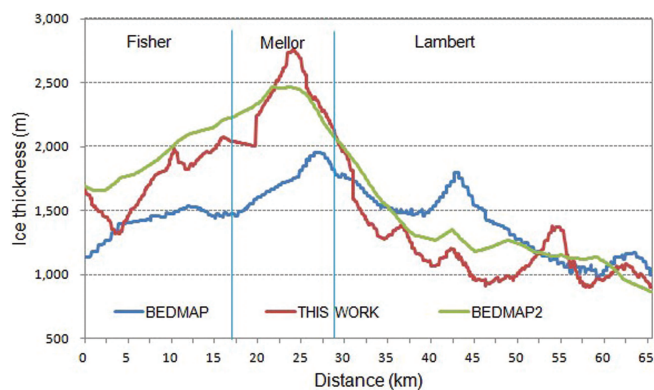


Fig. 3. Comparison of the ice thickness along the grounding line as indicated by the combined BEDMAP+PCMEGA dataset with BEDMAP and BEDMAP2 alone.

techniques and results in a directional bias in the grid (Lythe and others, 2001; Herzfeld, 2004). We first generate a net of 500 m × 500 m rectangular cells using a fishnet function of ArcGIS. We then average the coordinates and the ice thickness at all measurement points within each cell, independently for PCMEGA and for BEDMAP (Liu and others, 2007). After data processing, a total of 1226 ice thickness points are retained, including 811 points from PCMEGA and 415 points from BEDMAP. In the confluence region of the three glaciers, the density of ice thickness data points increased significantly (cf. BEDMAP alone) due to the addition of the PCMEGA ice thickness dataset. Before gridding the ice thickness, all data points within the outcrops and nunataks derived from BEDMAP2 products (Fretwell and others, 2013) are set to zero ice thickness and can be used for constructing the ice thickness grid as fixed points for grid interpolations. Finally, the ice thickness data are merged and interpolated onto a 400 m cell-size ice thickness grid using ordinary kriging (Fig. 2).

Preliminary error analysis is performed using the subsetting and validation tool in ArcGIS. Our 1226 sample points were randomly divided into two groups, including 1128 sample points for a training dataset and 98 points for a test dataset. The training dataset is used to generate an ice thickness grid applying ordinary kriging, and a root-mean-square error (RMSE) of 46 m was calculated by comparing the predictions with the known values in the test dataset.

Ice thickness characteristics

From Figure 2 several features can be observed. The thickest ice in the region is 2790 m, within the Mellor Glacier flowband of the ice shelf, and the thickest ice along the southern grounding line is 2760 m, at the transition zone of Mellor Glacier with the floating ice shelf. Of the three glaciers, Mellor and its flowband is thickest, mostly up to 2000 m, with some areas as thick as 2500 m. The ice thickness increases rapidly downstream of the Lambert Glacier/ice-shelf grounding line, from 1000–1500 to 1500–2000 m.

A comparison of the ice thickness along the southern grounding line as indicated by the combined BEDMAP+PCMEGA dataset with that indicated by BEDMAP alone shows that the combined dataset indicates Fisher Glacier is ~0–500 m thicker than indicated by BEDMAP, Mellor Glacier is ~300–1000 m thicker and Lambert Glacier is ~0–500 m thinner (Fig. 3). The ice thickness variability in

Table 1. Accumulation, ice flux and mass budget for Lambert, Mellor and Fisher glaciers, and for the total (Lambert basin)

Drainage basin	Area km ²	Total accumulation Gt a ⁻¹	Flux Gt a ⁻¹	Net budget Gt a ⁻¹	Flux based on BEDMAP2	Flux from Wen and others (2007)* Gt a ⁻¹	Flux from Yu and others (2010) [†] Gt a ⁻¹
Lambert	424 930	18.2 ± 1.3	14.0 ± 1.7	4.2 ± 2.3	15.4 ± 1.8	25.4 ± 2.5	19.0 ± 2.8
Mellor	448 590	16.3 ± 1.1	16.7 ± 2.0	-0.4 ± 2.6	16.7 ± 2.0	20.9 ± 2.1	14.9 ± 1.8
Fisher	97 090	4.7 ± 0.3	5.6 ± 0.6	-0.9 ± 0.8	6.2 ± 0.6	7.7 ± 0.8	5.0 ± 0.3
Total	970 610	39.2 ± 2.7	36.3 ± 2.7	2.9 ± 3.6	38.3 ± 2.8	54.0 ± 5.4	38.9 ± 3.3

*Flux based on hydrostatically derived ice thickness (Wen and others, 2007, table 3).

[†]Flux based on BEDMAP ice thickness (Yu and others, 2010, table 4).

the combined dataset is greater than that of BEDMAP, and more ice thickness detail along the grounding line is evident in the combined dataset. In contrast, a comparison of the ice thickness produced by the combined BEDMAP+PCMEGA dataset with BEDMAP2 shows that both datasets have a similar variation trend along the southern grounding line (Fig. 3), though the difference between the two datasets is still large (>300 m in some sections). This may be attributed to the different interpolation methods: BEDMAP2 initially gridded the in situ measurements of ice thickness at 5 km, then resampled the 5 km grid to a 1 km grid (Fretwell and others, 2013).

Mass budget of individual glaciers and of Lambert basin

We use the component approach (ISMASS Committee, 2004) to assess the mass budget and basal melting of the central portion of the Lambert–Amery system. We use velocity magnitude and azimuth data at 400 m × 400 m spacing from the MAMM project (Jezek, 2003, 2008) and resolve them normal to the grounding line. Ice volume flux F through the southern grounding line is calculated as the product of mean ice velocity and mean ice thickness at the grounding line (Wen and others, 2006):

$$F = \int K(w)R(w)H(w)U(w) dw \quad (1)$$

where H is the ice thickness, U is the surface ice velocity, w is the distance across the gate, $K = \sin \Phi$ is a correction factor applied to convert the velocity to its equivalent value normal to the gate (Φ is the angle between the gate and the ice flow direction) and R is the velocity ratio, which is assumed to be 1 along the grounding line where basal sliding makes up a substantial fraction of the column-averaged velocity (Huybrechts, 2002). The ice density (914 kg m⁻³) is used to convert the ice volume flux to mass flux.

The total snow water equivalent accumulated over the area upstream of the grounding line is estimated using the SMB dataset for the Antarctic ice sheet based on output of a regional atmospheric climate model RACMO2.1/ANT (Lenaerts and others, 2012). The differences between the accumulation (input) and the flux (output) are the mass budgets of the areas (in this case, Lambert Glacier, Mellor Glacier, Fisher Glacier and the total, which is equivalent to the Lambert basin; Table 1). Ice fluxes for the glaciers and the Lambert basin, based on BEDMAP2 (Fretwell and others, 2013), hydrostatically derived ice thickness (Wen and others, 2007) and BEDMAP (Yu and others, 2010), are also listed in Table 1 for comparison.

Our ice fluxes through the grounding lines of Lambert, Mellor and Fisher glaciers and of the Lambert basin as a whole are close to those of Yu and others (2010) and those based on BEDMAP2, except that our flux for Lambert Glacier is significantly less than that of Yu and others (2010) (Table 1). Our total surface accumulations for Lambert, Mellor and Fisher glaciers and over the Lambert basin as a whole are significantly less than those of Wen and others (2007, table 3) based on the average of the Vaughan and Giovinetto compilations (Vaughan and others, 1999; Giovinetto and Zwally, 2000), and those of Yu and others (2010, table 2) based on Vaughan and others (1999). For example, our total surface accumulation for the Lambert basin (39.2 ± 2.7 Gt a⁻¹) is only about two-thirds (51.4 ± 3.6 and 51.6 ± 2.6 Gt a⁻¹) those of Wen and others (2007) and Yu and others (2010) respectively. The results indicate that Mellor and Fisher glaciers are approximately in mass balance to the level of our measurement uncertainty, while Lambert Glacier is in positive imbalance. The three glaciers as a whole (Lambert basin), with a net mass budget of 2.9 ± 3.6 Gt a⁻¹, are approximately in mass balance to the level of our measurement uncertainty.

Basal melting estimates for the central flowband of the Amery Ice Shelf

Wen and others (2007) placed 18 flux gates along the Lambert, Mellor and Fisher flowbands, and estimated the basal melting and refreezing along the central flowband in detail. Here we use flux gates GL (the southern grounding line), G1 (~40 km downstream of the southern limit of the grounding line; Figs 1b and 2) and G18 (~10 km south of the ice-shelf front; fig. 2 of Wen and others, 2007) to provide an estimate of basal melting near the confluence of the three glaciers at the southern grounding line, and along the central flowband of the ice shelf. King and others (2009) suggest the Amery Ice Shelf has been relatively stable over four decades since 1968. In a similar fashion to Rignot (2002), Rignot and Jacobs (2002) and Wen and others (2007, 2010), the snow accumulation input and ice fluxes through the southern grounding line and the gates deployed over the ice shelf are used to estimate basal melting or refreezing, assuming the ice shelf is in a state of mass balance. The ice density (914 kg m⁻³) is also used to convert the ice volume melting to mass melting.

Net basal melt amount and average melt rate for the two sections (GL–G1 and G1–G18) of the ice-shelf central flowband and as a whole are presented in Table 2. The total basal melt amount in the region between the southern grounding line and flux gate G1 is estimated to be 5.4 ± 3.1 Gt a⁻¹, and

Table 2. Basal melting for the central flowband of the Amery Ice Shelf

Section	Accumulation Gt a ⁻¹	Influx from upstream Gt a ⁻¹	Outflux to downstream Gt a ⁻¹	Total basal melting Gt a ⁻¹	Area km ²	Average basal melting rate* m.w.e. a ⁻¹
GL–G1	0.0	36.3 ± 2.7	30.9 ± 1.5	5.4 ± 3.1	1043	5.2 ± 3.0 (21.0 ± 3.2)
G1–G18	3.4 ± 0.2	30.9 ± 1.5	18.6 ± 0.9	15.7 ± 1.8	21 531	0.7 ± 0.10 (0.8 ± 0.1)
GL–G18	3.4 ± 0.2	36.3 ± 2.7	18.6 ± 0.9	21.1 ± 2.9	22 574	0.9 ± 0.10 (1.8 ± 0.3)

*Values in parentheses were estimated using the ice thickness data from Wen and others (2007).

the average melting rate is $5.1 \pm 3.0 \text{ m a}^{-1}$ (Table 2). This melt rate is $\sim 25\%$ of the value ($21.0 \pm 3.2 \text{ m a}^{-1}$) calculated by Wen and others (2007), and $<20\%$ of the value ($31 \pm 5 \text{ m a}^{-1}$) calculated by Rignot and Jacobs (2002). Our net melt rate between G1 and G18 is $0.7 \pm 0.1 \text{ m a}^{-1}$, which is close to that estimated using the data from Wen and others (2007). The average melt rate of the whole central flowband of the Amery Ice Shelf is $0.9 \pm 0.1 \text{ m a}^{-1}$, less than estimated ($1.8 \pm 0.3 \text{ m a}^{-1}$), using the data from Wen and others (2007). We believe the differences in these results are primarily caused by the substantially different ice thickness values used along the southern grounding line; previous studies used hydrostatically derived ice thickness data.

The error sources in our mass-balance estimates include uncertainties in accumulation and ice flux. We assume a 5% accumulation rate error and 5% area error (Yu and others, 2010). The estimated accuracy of the ice velocity data is $\pm 10 \text{ m a}^{-1}$ (Jezek, 2003, 2008); the mean difference between the InSAR velocities and the GPS velocity measurements is $4.41 \pm 9.7 \text{ m a}^{-1}$ (Wen and others, 2010). The uncertainty of the velocity azimuth is 3° (Yu and others, 2010). The ice thickness error from PCMEGA is up to 50 m (Damm, 2007) and BEDMAP error ranges from 30 to 100 m (Lythe and others, 2001; Yu and others, 2010). Our ice thickness grid has an RMSE of 46 m, estimated by comparing the predictions with the known values in the test dataset. The errors in the ice flux, mass budget and basal melting estimates are quantified, based on statistical theory of error propagation (Taylor, 1997; Tables 1 and 2).

DISCUSSION AND CONCLUSION

Our analysis indicates that the ice flux through the Amery Ice Shelf southern grounding line is $36.3 \pm 2.7 \text{ Gt a}^{-1}$, which is close to the value ($38.9 \pm 3.3 \text{ Gt a}^{-1}$) of Yu and others (2010), but much less than that ($54.0 \pm 5.4 \text{ Gt a}^{-1}$) of Wen and others (2007). Mellor and Fisher Glaciers are approximately in mass balance to the level of our measurement uncertainty, while Lambert Glacier has a positive imbalance of $4.2 \pm 2.3 \text{ Gt a}^{-1}$. The overall mass budget ($2.9 \pm 3.6 \text{ Gt a}^{-1}$) for the Lambert Glacier basin is approximately in mass balance to the level of our measurement uncertainty, which is similar to the result of Shepherd and others (2012, fig. 1), who used the same SMB dataset as Lenaerts and others (2012). The overall mass budget for the Lambert Glacier basin is also similar to the results of Rignot (2002), Wen and others (2007) and Rignot and others (2008), but previous total snow accumulations and ice fluxes across the southern grounding line are much larger than those used in this study. The overall mass budget for the Lambert Glacier basin is different from the result of Yu and others (2010) who found a significantly positive imbalance. This is

because the new SMB dataset (Lenaerts and others, 2012) indicates lower net snow accumulation over the Lambert basin than that of Vaughan and others (1999), and used by Yu and others (2010). Based on satellite remote sensing and field-gathered datasets, Scambos and others (2012) found that there is a large extent of near-zero net surface accumulation 'wind glaze' areas on the East Antarctic plateau, resulting from persistent katabatic winds. Studies of SMB (e.g. Vaughan and others, 1999; Giovinetto and Zwally, 2000) interpolate values across glaze regions, leading to overestimates of net mass input. Of three recent models of Antarctic SMB, the lowest-input model (Lenaerts and others, 2012) appears to best match the mean in regions of extensive wind glaze (Scambos and others, 2012). The Lambert Glacier basin has a large percentage (19.1%) of glaze area above 1500 m elevation, leading to a much lower total snow accumulation than previous estimates (e.g. Rignot, 2002; Wen and others, 2007; Rignot and others, 2008; Yu and others, 2010).

The average melt rate for the region between the southern grounding line and flux gate G1 is $5.1 \pm 3.0 \text{ m a}^{-1}$, which is less than the estimate ($10.4 \pm 2.4 \text{ m a}^{-1}$) of Yu and others (2010) and less, by 20–25%, than the results of Rignot (2002), Rignot and Jacobs (2002) and Wen and others (2007). The differences are primarily caused by the use of different ice thickness datasets at the southern grounding line flux gates, where both Rignot (2002) and Wen and others (2007) used hydrostatically derived ice thickness data while we (and Yu and others, 2010) used RES ice thickness measurements. Because of ice flexure due to tidal movement at the grounding zone, the hydrostatic equilibrium condition between elevation and ice thickness is not satisfied in the confluence zone (Fricker and others, 2009). The hydrostatic method may therefore overestimate ice thickness in this zone (Yu and others, 2010), resulting in high ice flux estimates. Our study combines the RES ice thickness data from BEDMAP and PCMEGA to generate a digital ice thickness grid over the Amery Ice Shelf southern grounding zone region, to further reduce the uncertainty in the ice thickness data used by Yu and others (2010).

ACKNOWLEDGEMENTS

This work is supported by the National Natural Science Foundation of China (grant No. 41276188) and National Basic Research Program of China (grant No. 2012CB957704). We thank J.T.M. Lenaerts for providing SMB data, Jaehyung Yu and Hongxing Liu for providing the interpolated ice thickness grid and T.A. Scambos for valuable comments. Constructive comments and suggestions from two anonymous reviewers have been very helpful in improving this paper.

REFERENCES

- Allison I (1979) The mass budget of the Lambert Glacier drainage basin, Antarctica. *J. Glaciol.*, **22**(87), 223–235
- Bentley CR and Giovinetto MB (1991) Mass balance of Antarctica and sea level change. In Weller G, Wilson CL and Severin BAB eds. *Proceedings of International Conference on the Role of the Polar Regions in Global Change, Vol. 2*. University of Alaska Fairbanks, Fairbanks, AK, 481–488
- Bindschadler R and 17 others (2011) Getting around Antarctica: new high-resolution mappings of the grounded and freely-floating boundaries of the Antarctic ice sheet created for the International Polar Year. *Cryosphere*, **5**(3), 569–588 (doi: 10.5194/tc-5-569-2011)
- Budd WF, Corry MJ and Jacka TH (1982) Results from the Amery Ice Shelf Project. *Ann. Glaciol.*, **3**, 36–41
- Damm V (2007) A subglacial topographic model of the southern drainage area of the Lambert Glacier/Amery Ice Shelf system: results of an airborne ice thickness survey south of the Prince Charles Mountains. *Terra Antart.*, **14**(1), 85–94
- Fretwell P and 59 others (2013) Bedmap2: improved ice bed, surface and thickness datasets for Antarctica. *Cryosphere*, **7**(1), 375–393 (doi: 10.5194/tc-7-375-2013)
- Fricker HA, Warner RC and Allison I (2000) Mass balance of the Lambert Glacier–Amery Ice Shelf system, East Antarctica: a comparison of computed balance fluxes and measured fluxes. *J. Glaciol.*, **46**(155), 561–570 (doi: 10.3189/172756500781832765)
- Fricker HA, Coleman R, Padman L, Scambos TA, Bohlander J and Brunt KM (2009) Mapping the grounding zone of the Amery Ice Shelf, East Antarctica using InSAR, MODIS and ICESat. *Antarct. Sci.*, **21**(5), 515–532 (doi: 10.1017/S095410200999023X)
- Galton-Fenzi BK, Hunter JR, Coleman J, Marsland SJ and Warner RC (2012) Modeling the basal melting and marine ice accretion of the Amery Ice Shelf. *J. Geophys. Res.*, **117**(C9), C09031 (doi: 10.1029/2012JC008214)
- Giovinetto MB and Zwally HJ (2000) Spatial distribution of net surface accumulation on the Antarctic ice sheet. *Ann. Glaciol.*, **31**, 171–178
- Herzfeld UC (2004) *Atlas of Antarctica: topographic maps from geostatistical analysis of satellite radar altimeter data*. Springer, Berlin
- Huybrechts P (2002) Sea-level changes at the LGM from ice-dynamic reconstructions of the Greenland and Antarctic ice sheets during the glacial cycles. *Quat. Sci. Rev.*, **21**(1–3), 203–231 (doi: 10.1016/S0277-3791(01)00082-8)
- ISMSS Committee (2004) Recommendations for the collection and synthesis of Antarctic ice sheet mass balance data. *Global Planet. Change*, **42**(1–4), 1–15
- Jezek KC (2002) RADARSAT-1 Antarctic Mapping Project: change-detection and surface velocity campaign. *Ann. Glaciol.*, **34**, 263–268 (doi: 10.3189/172756402781818030)
- Jezek KC (2003) Observing the Antarctic ice sheet using the RADARSAT-1 synthetic aperture radar. *Polar Geogr.*, **27**(3), 197–209 (doi: 10.1080/789610167)
- Jezek KC (2008) *The RADARSAT-1 Antarctic Mapping Project*. (BPRC Report No. 22) Byrd Polar Research Center, Ohio State University, Columbus, OH
- King MA (2002) The dynamics of the Amery Ice Shelf from a combination of terrestrial and space geodetic data. (PhD thesis, University of Tasmania)
- King MA, Coleman R, Morgan PJ and Hurd RS (2007) Velocity change of the Amery Ice Shelf, East Antarctica, during the period 1968–1999. *J. Geophys. Res.*, **112**(F1), F01013 (doi: 10.1029/2006JF000609)
- King MA and 7 others (2009) A 4-decade record of elevation change of the Amery Ice Shelf, East Antarctica. *J. Geophys. Res.*, **114**(F1), F01010 (doi: 10.1029/2008JF001094)
- Lenaerts JTM, Van den Broeke MR, Van de Berg WJ, Van Meijgaard E and Kuipers Munneke P (2012) A new, high-resolution surface mass balance map of Antarctica (1979–2010) based on regional atmospheric climate modeling. *Geophys. Res. Lett.*, **39**(4), L04501 (doi: 10.1029/2011GL050713)
- Liu J, Wen J, Wang Y, Wang W, Csatho BM and Jezek KC (2007) Development and applications of Dome A-DEM in Antarctic Ice Sheet. *Chinese Geogr. Sci.*, **17**(2), 160–165 (doi: 10.1007/s11769-007-0160-4)
- Lythe MB, Vaughan DG and BEDMAP consortium (2001) BEDMAP: a new ice thickness and subglacial topographic model of Antarctica. *J. Geophys. Res.*, **106**(B6), 11 335–11 351 (doi: 10.1029/2000JB900449)
- McIntyre NF (1985) A re-assessment of the mass balance of the Lambert Glacier drainage basin, Antarctica. *J. Glaciol.*, **31**(107), 34–38
- Rignot E (2002) Mass balance of East Antarctic glaciers and ice shelves from satellite data. *Ann. Glaciol.*, **34**, 217–227 (doi: 10.3189/172756402781817419)
- Rignot E and Jacobs SS (2002) Rapid bottom melting widespread near Antarctic ice sheet grounding lines. *Science*, **296**(5575), 2020–2023 (doi: 10.1126/science.1070942)
- Rignot E and 6 others (2008) Recent Antarctic ice mass loss from radar interferometry and regional climate modelling. *Nature Geosci.*, **1**(2), 106–110 (doi: 10.1038/ngeo102)
- Rignot E, Mouginot J and Scheuchl B (2011) Antarctic grounding line mapping from differential satellite radar interferometry. *Geophys. Res. Lett.*, **38**(10), L10504 (doi: 10.1029/2011GL047109)
- Scambos TA and 12 others (2012) Extent of low-accumulation ‘wind glaze’ areas on the East Antarctic plateau: implications for continental ice mass balance. *J. Glaciol.*, **58**(210), 633–647 (doi: 10.3189/2012JoG11J232)
- Shepherd A and 46 others (2012) A reconciled estimate of ice-sheet mass balance. *Science*, **338** (6111), 1183–1189 (doi: 10.1126/science.1228102)
- Taylor JR (1997) *An introduction to error analysis: the study of uncertainties in physical measurements*, 2nd edn. University Science Books, Sausalito, CA
- Vaughan DG, Bamber JL, Giovinetto MB, Russell J and Cooper APR (1999) Reassessment of net surface mass balance in Antarctica. *J. Climate*, **12**(4), 933–946 (doi: 10.1175/1520-0442(1999)012<0933:RONSMB>2.0.CO;2)
- Wen J, Jezek KC, Monaghan AJ, Sun B, Ren J and Huybrechts P (2006) Accumulation variability and mass budgets of the Lambert Glacier–Amery Ice Shelf system, East Antarctica, at high elevations. *Ann. Glaciol.*, **43**, 351–360 (doi: 10.3189/172756406781812249)
- Wen J, Jezek KC, Csatho B, Herzfeld UC, Farness KL and Huybrechts P (2007) Mass budgets of the Lambert, Mellor and Fisher Glaciers and basal fluxes beneath their flowbands on Amery Ice Shelf. *Sci. China D*, **50**(11), 1693–1706 (doi: 10.1007/s11430-007-0120-y)
- Wen J, Wang Y, Wang W, Jezek KC, Liu H and Allison I (2010) Basal melting and freezing under the Amery Ice Shelf, East Antarctica. *J. Glaciol.*, **56**(195), 81–90 (doi: 10.3189/002214310791190820)
- Yu J, Liu H, Jezek KC, Warner RC and Wen J (2010) Analysis of velocity field, mass balance, and basal melt of the Lambert Glacier–Amery Ice Shelf system by incorporating Radarsat SAR interferometry and ICESat laser altimetry measurements. *J. Geophys. Res.*, **115**(B11), B11102 (doi: 10.1029/2010JB007456)